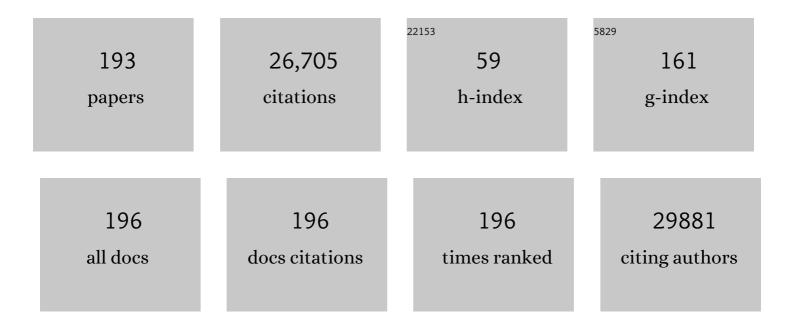
Yumeng Shi

List of Publications by Year in descending order

Source: https://exaly.com/author-pdf/7000200/publications.pdf Version: 2024-02-01



YUMENC SHI

#	Article	IF	CITATIONS
1	Wafer-scale single-orientation 2D layers by atomic edge-guided epitaxial growth. Chemical Society Reviews, 2022, 51, 803-811.	38.1	18
2	A convergent paired electrolysis strategy enables the cross-coupling of methylarenes with imines. Organic Chemistry Frontiers, 2022, 9, 2193-2197.	4.5	6
3	Two-Dimensional Cs ₂ AgBiBr ₆ /WS ₂ Heterostructure-Based Photodetector with Boosted Detectivity via Interfacial Engineering. ACS Nano, 2022, 16, 3985-3993.	14.6	49
4	Efficient red photoluminescence in holmium-doped Cs2NaInCl6 double perovskite. Cell Reports Physical Science, 2022, 3, 100820.	5.6	31
5	Chiral Ligand-Induced Structural Transformation of Low-Dimensional Hybrid Perovskite for Circularly Polarized Photodetection. Chemistry of Materials, 2022, 34, 2955-2962.	6.7	24
6	Ultrafast growth of high-quality large-sized GaSe crystals by liquid metal promoter. Nano Research, 2022, 15, 4677-4681.	10.4	14
7	Efficient energy transfer in organic light-emitting transistor with tunable wavelength. Nano Research, 2022, 15, 3647-3652.	10.4	5
8	Co/Fe ₃ O ₄ nanoparticles embedded in N-doped hierarchical porous carbon derived from zeolitic imidazolate frameworks as efficient oxygen reduction electrocatalysts for zinc–air battery-based desalination. Journal of Materials Chemistry A, 2022, 10, 12213-12224.	10.3	12
9	A Novel 4,4'-Bipiperidine-Based Organic Salt for Efficient and Stable 2D-3D Perovskite Solar Cells. ACS Applied Materials & Interfaces, 2022, 14, 22324-22331.	8.0	6
10	Recent advances in kinetic optimizations of cathode materials for rechargeable magnesium batteries. Coordination Chemistry Reviews, 2022, 466, 214597.	18.8	19
11	Highly Reversible Moistureâ€Induced Bright Selfâ€Trapped Exciton Emissions in a Copperâ€Based Organic–Inorganic Hybrid Metal Halide. Advanced Optical Materials, 2022, 10, .	7.3	12
12	Efficient Multicolor and White Photoluminescence in Erbium- and Holmium-Incorporated Cs ₂ NaInCl ₆ :Sb ³⁺ Double Perovskites. Chemistry of Materials, 2022, 34, 6288-6295.	6.7	49
13	Low-defect-density WS2 by hydroxide vapor phase deposition. Nature Communications, 2022, 13, .	12.8	37
14	Efficient low-frequency microwave absorption and solar evaporation properties of γ-Fe2O3 nanocubes/graphene composites. Chemical Engineering Journal, 2021, 405, 126676.	12.7	63
15	A Scalable H ₂ O–DMF–DMSO Solvent Synthesis of Highly Luminescent Inorganic Perovskiteâ€Related Cesium Lead Bromides. Advanced Optical Materials, 2021, 9, 2001435.	7.3	16
16	Design of Black Phosphorous Derivatives with Excellent Stability and Ion-Kinetics for Alkali Metal-Ion Battery. Energy Storage Materials, 2021, 35, 283-309.	18.0	8
17	Mechanism investigation of high performance Na3V2(PO4)2O2F/reduced graphene oxide cathode for sodium-ion batteries. Journal of Power Sources, 2021, 482, 228906.	7.8	27
18	Redox-catalysis flow electrode desalination in an organic solvent. Journal of Materials Chemistry A, 2021, 9, 22254-22261.	10.3	18

Yumeng Shi

#	Article	IF	CITATIONS
19	Highly efficient and stable ionic liquid-based gel electrolytes. Nanoscale, 2021, 13, 7140-7151.	5.6	11
20	Unveiling the Relationship between the Surface Chemistry of Nanoparticles and Ion Transport Properties of the Resulting Composite Electrolytes. Journal of Physical Chemistry Letters, 2021, 12, 642-649.	4.6	4
21	2D Cs ₂ AgBiBr ₆ with Boosted Light–Matter Interaction for Highâ€Performance Photodetectors. Advanced Optical Materials, 2021, 9, 2001930.	7.3	42
22	A Scalable H ₂ O–DMF–DMSO Solvent Synthesis of Highly Luminescent Inorganic Perovskiteâ€Related Cesium Lead Bromides (Advanced Optical Materials 3/2021). Advanced Optical Materials, 2021, 9, 2170012.	7.3	1
23	In Situ Synthesis of Lead-Free Halide Perovskite Cs ₂ AgBiBr ₆ Supported on Nitrogen-Doped Carbon for Efficient Hydrogen Evolution in Aqueous HBr Solution. ACS Applied Materials & Interfaces, 2021, 13, 10037-10046.	8.0	52
24	MXeneâ€Based Materials for Electrochemical Sodiumâ€Ion Storage. Advanced Science, 2021, 8, e2003185.	11.2	88
25	Unlocking Rapid and Robust Sodium Storage Performance of Zinc-Based Sulfide <i>via</i> Indium Incorporation. ACS Nano, 2021, 15, 8507-8516.	14.6	36
26	Rational design of MXene-based films for energy storage: Progress, prospects. Materials Today, 2021, 46, 183-211.	14.2	83
27	Supramolecular engineering of charge transfer in wide bandgap organic semiconductors with enhanced visible-to-NIR photoresponse. Nature Communications, 2021, 12, 3667.	12.8	30
28	Porosity Engineering of MXene Membrane towards Polysulfide Inhibition and Fast Lithium Ion Transportation for Lithium–Sulfur Batteries. Small, 2021, 17, e2007442.	10.0	57
29	One-Dimensional Organic–Metal Halide with Highly Efficient Warm White-Light Emission and Its Moisture-Induced Structural Transformation. Chemistry of Materials, 2021, 33, 5668-5674.	6.7	30
30	Efficient White Photoluminescence from Self-Trapped Excitons in Sb ³⁺ /Bi ³⁺ -Codoped Cs ₂ NaInCl ₆ Double Perovskites with Tunable Dual-Emission. ACS Energy Letters, 2021, 6, 3343-3351.	17.4	126
31	Harmonic generation in transition metal dichalcogenides and their heterostructures. Materials Today, 2021, 50, 570-586.	14.2	14
32	Highly Efficient Whiteâ€Light Emission Triggered by Sb ³⁺ Dopant in Indiumâ€Based Double Perovskites. Advanced Photonics Research, 2021, 2, 2100143.	3.6	15
33	Zeroâ€Dimensional Organic–Inorganic Hybrid Copperâ€Based Halides with Highly Efficient Orange–Red Emission. Small, 2021, 17, e2103831.	10.0	25
34	Towards Dendriteâ€Free Potassiumâ€Metal Batteries: Rational Design of a Multifunctional 3D Polyvinyl Alcoholâ€Borax Layer. Angewandte Chemie - International Edition, 2021, 60, 25122-25127.	13.8	32
35	Towards Dendriteâ€Free Potassiumâ€Metal Batteries: Rational Design of a Multifunctional 3D Polyvinyl Alcoholâ€Borax Layer. Angewandte Chemie, 2021, 133, 25326-25331.	2.0	4
36	Surface Charge Transfer Doping Enabled Large Hysteresis in van der Waals Heterostructures for Artificial Synapse. , 2021, 3, 235-242.		14

#	Article	IF	CITATIONS
37	Suppressing Li Dendrite Puncture with a Hierarchical h-BN Protective Layer. ACS Applied Materials & Interfaces, 2021, 13, 56109-56115.	8.0	9
38	Nanocarbon Catalysts: Recent Understanding Regarding the Active Sites. Advanced Science, 2020, 7, 1902126.	11.2	94
39	Synthesis of bismuth sulfide nanobelts for high performance broadband photodetectors. Journal of Materials Chemistry C, 2020, 8, 2102-2108.	5.5	43
40	Enhanced sodium storage kinetics by volume regulation and surface engineering <i>via</i> rationally designed hierarchical porous FeP@C/rGO. Nanoscale, 2020, 12, 4341-4351.	5.6	80
41	Constructing stress-release layer on Fe7Se8-based composite for highly stable sodium-storage. Nano Energy, 2020, 69, 104389.	16.0	49
42	High speed capacitive deionization system with flow-through electrodes. Desalination, 2020, 496, 114750.	8.2	19
43	Quantum dot-carbonaceous nanohybrid composites: preparation and application in electrochemical energy storage. Journal of Materials Chemistry A, 2020, 8, 22488-22506.	10.3	26
44	Enhanced ambipolar charge transport for efficient organic single crystal light-emitting transistors with a narrowed ambipolar regime. Journal of Materials Chemistry C, 2020, 8, 16333-16338.	5.5	9
45	Nanoframes@CNT Beadsâ€onâ€aâ€String Structures: Toward an Advanced Highâ€Stable Sodiumâ€Ion Full Battery. Small, 2020, 16, e2005095.	10.0	15
46	Stepwise Intercalation-Conversion-Intercalation Sodiation Mechanism in CuInS ₂ Prompting Sodium Storage Performance. ACS Energy Letters, 2020, 5, 3725-3732.	17.4	33
47	Stimuliâ€Enabled Artificial Synapses for Neuromorphic Perception: Progress and Perspectives. Small, 2020, 16, e2001504.	10.0	55
48	3D printed rGO/CNT microlattice aerogel for a dendrite-free sodium metal anode. Journal of Materials Chemistry A, 2020, 8, 19843-19854.	10.3	82
49	Photocatalytic Hydrogen Evolution: Photocatalytic Hydrogen Evolution under Ambient Conditions on Polymeric Carbon Nitride/Donorâ€i€â€Acceptor Organic Molecule Heterostructures (Adv. Funct.) Tj ETQq1 1	0.7849314	rg&T /Overic
50	Facile and Reversible Carrier-Type Manipulation of Layered MoTe ₂ Toward Long-Term Stable Electronics. ACS Applied Materials & Interfaces, 2020, 12, 42918-42924.	8.0	4
51	Photocatalytic Hydrogen Evolution under Ambient Conditions on Polymeric Carbon Nitride/Donorâ€i€â€Acceptor Organic Molecule Heterostructures. Advanced Functional Materials, 2020, 30, 2005106.	14.9	46
52	Sb nanoparticle decorated rGO as a new anode material in aqueous chloride ion batteries. Nanoscale, 2020, 12, 12268-12274.	5.6	20
53	Zinc–Air Battery-Based Desalination Device. ACS Applied Materials & Interfaces, 2020, 12, 25728-25735.	8.0	29
54	Photocathode-assisted redox flow desalination. Green Chemistry, 2020, 22, 4133-4139.	9.0	29

#	Article	IF	CITATIONS
55	Lithiophilic Silver Coating on Lithium Metal Surface for Inhibiting Lithium Dendrites. Frontiers in Chemistry, 2020, 8, 109.	3.6	16

56 Nanocarbon Catalysts: Nanocarbon Catalysts: Recent Understanding Regarding the Active Sites (Adv.) Tj ETQq0 0 0 rgBT /Overlock 10 T

57	Rapid synthesis and mechanochemical reactions of cesium copper halides for convenient chromaticity tuning and efficient white light emission. Journal of Materials Chemistry C, 2020, 8, 4895-4901.	5.5	49
58	Rechargeable Aqueous Zinc-Ion Batteries in MgSO4/ZnSO4 Hybrid Electrolytes. Nano-Micro Letters, 2020, 12, 60.	27.0	60
59	Photoluminescence Mechanisms of Allâ€Inorganic Cesium Lead Bromide Perovskites Revealed by Single Particle Spectroscopy. ChemNanoMat, 2020, 6, 327-335.	2.8	16
60	Grain Boundary Induced Ultralow Threshold Random Laser in a Single GaTe Flake. ACS Applied Materials & Interfaces, 2020, 12, 23323-23329.	8.0	10
61	Morphological and Electronic Dual Regulation of Cobalt–Nickel Bimetal Phosphide Heterostructures Inducing High Water-Splitting Performance. Journal of Physical Chemistry Letters, 2020, 11, 3911-3919.	4.6	33
62	Defect-induced nucleation and epitaxial growth of a MOF-derived hierarchical Mo ₂ C@Co architecture for an efficient hydrogen evolution reaction. RSC Advances, 2020, 10, 13838-13847.	3.6	7
63	Boosting chem-insertion and phys-adsorption in S/N co-doped porous carbon nanospheres for high-performance symmetric Li-ion capacitors. Journal of Materials Chemistry A, 2020, 8, 11529-11537.	10.3	30
64	Controllable nonlinear optical properties of different-sized iron phosphorus trichalcogenide (FePS3) nanosheets. Nanophotonics, 2020, 9, 4555-4564.	6.0	9
65	Postâ€Treatment of CH ₃ NH ₃ PbI ₃ /PbI ₂ Composite Films with Methylamine to Realize Highâ€Performance Photoconductor Devices. Chemistry - an Asian Journal, 2019, 14, 2861-2868.	3.3	7
66	Defective NiFe ₂ O ₄ Nanoparticles for Efficient Urea Electroâ€oxidation. Chemistry - an Asian Journal, 2019, 14, 2796-2801.	3.3	14
67	An Aqueous Rechargeable Fluoride Ion Battery with Dual Fluoride Electrodes. Journal of the Electrochemical Society, 2019, 166, A2419-A2424.	2.9	19
68	Template growth of perovskites on yarn fibers induced by capillarity for flexible photoelectric applications. Journal of Materials Chemistry C, 2019, 7, 9496-9503.	5.5	12
69	Self-Powered Perovskite/CdS Heterostructure Photodetectors. ACS Applied Materials & Interfaces, 2019, 11, 40204-40213.	8.0	65
70	Dendrite-Free Li Metal Plating/Stripping Onto Three-Dimensional Vertical-Graphene@Carbon-Cloth Host. Frontiers in Chemistry, 2019, 7, 714.	3.6	24
71	High-Concentration Niobium-Substituted WS2 Basal Domains with Reconfigured Electronic Band Structure for Hydrogen Evolution Reaction. ACS Applied Materials & Interfaces, 2019, 11, 34862-34868.	8.0	21
72	Influence of the Organic Chain on the Optical Properties of Two-Dimensional Organic–Inorganic Hybrid Lead Iodide Perovskites. ACS Applied Electronic Materials, 2019, 1, 2253-2259.	4.3	13

#	Article	IF	CITATIONS
73	Boosting Sodium Storage of Fe1â^'xS/MoS2 Composite via Heterointerface Engineering. Nano-Micro Letters, 2019, 11, 80.	27.0	77
74	Effects of precursor pre-treatment on the vapor deposition of WS ₂ monolayers. Nanoscale Advances, 2019, 1, 953-960.	4.6	17
75	Effect of mechanical forces on thermal stability reinforcement for lead based perovskite materials. Journal of Materials Chemistry A, 2019, 7, 540-548.	10.3	26
76	The photoluminescence mechanism of CsPb ₂ Br ₅ microplates revealed by spatially resolved single particle spectroscopy. Nanoscale, 2019, 11, 3186-3192.	5.6	43
77	Location-selective growth of two-dimensional metallic/semiconducting transition metal dichalcogenide heterostructures. Nanoscale, 2019, 11, 4183-4189.	5.6	16
78	Polypyrrole coated niobium disulfide nanowires as high performance electrocatalysts for hydrogen evolution reaction. Nanotechnology, 2019, 30, 405601.	2.6	7
79	Toward the Growth of High Mobility 2D Transition Metal Dichalcogenide Semiconductors. Advanced Materials Interfaces, 2019, 6, 1900220.	3.7	42
80	In Situ Transmission Electron Microscopy for Energy Materials and Devices. Advanced Materials, 2019, 31, e1900608.	21.0	95
81	Construction of complex NiS multi-shelled hollow structures with enhanced sodium storage. Energy Storage Materials, 2019, 23, 17-24.	18.0	83
82	Bifunctional nickel oxide-based nanosheets for highly efficient overall urea splitting. Chemical Communications, 2019, 55, 6555-6558.	4.1	53
83	Continuous desalination with a metal-free redox-mediator. Journal of Materials Chemistry A, 2019, 7, 13941-13947.	10.3	38
84	Rhenium disulfide nanosheets/carbon composite as novel anodes for high-rate and long lifespan sodium-ion batteries. Nano Energy, 2019, 61, 626-636.	16.0	46
85	Base-enhanced electrochemical water oxidation by a nickel complex in neutral aqueous solution. Chemical Communications, 2019, 55, 6122-6125.	4.1	36
86	3D self-branched zinc-cobalt Oxide@N-doped carbon hollow nanowall arrays for high-performance asymmetric supercapacitors and oxygen electrocatalysis. Energy Storage Materials, 2019, 23, 653-663.	18.0	104
87	An all manganese-based oxide nanocrystal cathode and anode for high performance lithium-ion full cells. Nanoscale Advances, 2019, 1, 1714-1720.	4.6	7
88	High Oxidation Resistance of CVD Graphene-Reinforced Copper Matrix Composites. Nanomaterials, 2019, 9, 498.	4.1	16
89	High-Performance Photoresistors Based on Perovskite Thin Film with a High PbI2 Doping Level. Nanomaterials, 2019, 9, 505.	4.1	12
90	Tunable Pseudocapacitive Behavior in Metal–Organic Framework-Derived TiO ₂ @Porous Carbon Enabling High-Performance Membrane Capacitive Deionization. ACS Applied Energy Materials, 2019, 2, 1812-1822.	5.1	60

#	Article	IF	CITATIONS
91	Electrochemical Performance of Sb ₄ O ₅ Cl ₂ as a New Anode Material in Aqueous Chloride-Ion Battery. ACS Applied Materials & Interfaces, 2019, 11, 9144-9148.	8.0	44
92	Thermal-Assisted Vertical Electron Injections in Few-Layer Pyramidal-Structured MoS ₂ Crystals. Journal of Physical Chemistry Letters, 2019, 10, 1292-1299.	4.6	5
93	Promoting polysulfide conversion by catalytic ternary Fe ₃ O ₄ /carbon/graphene composites with ordered microchannels for ultrahigh-rate lithium–sulfur batteries. Journal of Materials Chemistry A, 2019, 7, 25078-25087.	10.3	68
94	Design Multifunctional Catalytic Interface: Toward Regulation of Polysulfide and Li ₂ S Redox Conversion in Li–S Batteries. Small, 2019, 15, e1906132.	10.0	62
95	An organic flow desalination battery. Energy Storage Materials, 2019, 20, 203-207.	18.0	47
96	Boosting the Electrocatalytic Water Oxidation Performance of CoFe ₂ O ₄ Nanoparticles by Surface Defect Engineering. ACS Applied Materials & Interfaces, 2019, 11, 3978-3983.	8.0	76
97	Significant photoluminescence enhancement in WS ₂ monolayers through Na ₂ S treatment. Nanoscale, 2018, 10, 6105-6112.	5.6	35
98	Efficient Sodium Storage in Rolledâ€Up Amorphous Si Nanomembranes. Advanced Materials, 2018, 30, e1706637.	21.0	87
99	MoS _x -coated NbS ₂ nanoflakes grown on glass carbon: an advanced electrocatalyst for the hydrogen evolution reaction. Nanoscale, 2018, 10, 3444-3450.	5.6	24
100	Bifunctional porous iron phosphide/carbon nanostructure enabled high-performance sodium-ion battery and hydrogen evolution reaction. Energy Storage Materials, 2018, 15, 98-107.	18.0	102
101	Epitaxial Growth of Two-Dimensional Layered Transition-Metal Dichalcogenides: Growth Mechanism, Controllability, and Scalability. Chemical Reviews, 2018, 118, 6134-6150.	47.7	285
102	Synthesis and optoelectronic applications of graphene/transition metal dichalcogenides flat-pack assembly. Carbon, 2018, 127, 602-610.	10.3	15
103	Direct Observation of Perovskite Photodetector Performance Enhancement by Atomically Thin Interface Engineering. ACS Applied Materials & Interfaces, 2018, 10, 36493-36504.	8.0	25
104	Recent advances of low-dimensional materials in lasing applications. FlatChem, 2018, 10, 22-38.	5.6	14
105	The electrochemical behaviors of NaF dual battery based on the hybrid electrodes of nano-bismuth@CNTs. Materials Letters, 2018, 233, 332-335.	2.6	8
106	3D carbon foam-supported WS ₂ nanosheets for cable-shaped flexible sodium ion batteries. Journal of Materials Chemistry A, 2018, 6, 10813-10824.	10.3	112
107	Tailoring NiO Nanostructured Arrays by Sulfate Anions for Sodiumâ€lon Batteries. Small, 2018, 14, e1800898.	10.0	39
108	Two-step fabrication of single-layer rectangular SnSe flakes. 2D Materials, 2017, 4, 021026.	4.4	57

#	Article	IF	CITATIONS
109	PAH contamination in road dust from a moderate city in North China: The significant role of traffic emission. Human and Ecological Risk Assessment (HERA), 2017, 23, 1072-1085.	3.4	16
110	Fe 2 O 3 nanothorns sensitized two-dimensional TiO 2 nanosheets for highly efficient solar energy conversion. FlatChem, 2017, 3, 1-7.	5.6	14
111	InGaN/GaN nanowires epitaxy on large-area MoS2 for high-performance light-emitters. RSC Advances, 2017, 7, 26665-26672.	3.6	32
112	Graphene-Au nanoparticle based vertical heterostructures: A novel route towards high- ZT Thermoelectric devices. Nano Energy, 2017, 38, 385-391.	16.0	26
113	Atomic-Monolayer Two-Dimensional Lateral Quasi-Heterojunction Bipolar Transistors with Resonant Tunneling Phenomenon. ACS Nano, 2017, 11, 11015-11023.	14.6	45
114	A review on the research progress of tailoring photoluminescence of monolayer transition metal dichalcogenides. FlatChem, 2017, 4, 48-53.	5.6	18
115	High-efficiency omnidirectional photoresponses based on monolayer lateral p–n heterojunctions. Nanoscale Horizons, 2017, 2, 37-42.	8.0	21
116	Promoting the yield and crystallinity of synthetic WS2 via precursor pretreatment. , 2017, , .		0
117	Determination of band offsets at GaN/single-layer MoS2 heterojunction. Applied Physics Letters, 2016, 109, .	3.3	64
118	Gap States at Low-Angle Grain Boundaries in Monolayer Tungsten Diselenide. Nano Letters, 2016, 16, 3682-3688.	9.1	55
119	Atomic-Monolayer MoS ₂ Band-to-Band Tunneling Field-Effect Transistor. Small, 2016, 12, 5676-5683.	10.0	41
120	Tracking Optical Welding through Groove Modes in Plasmonic Nanocavities. Nano Letters, 2016, 16, 5605-5611.	9.1	44
121	Strong Rashba-Edelstein Effect-Induced Spin–Orbit Torques in Monolayer Transition Metal Dichalcogenide/Ferromagnet Bilayers. Nano Letters, 2016, 16, 7514-7520.	9.1	247
122	Laterally Stitched Heterostructures of Transition Metal Dichalcogenide: Chemical Vapor Deposition Growth on Lithographically Patterned Area. ACS Nano, 2016, 10, 10516-10523.	14.6	52
123	Dual-mode operation of 2D material-base hot electron transistors. Scientific Reports, 2016, 6, 32503.	3.3	12
124	Heterostructured WS ₂ /CH ₃ NH ₃ PbI ₃ Photoconductors with Suppressed Dark Current and Enhanced Photodetectivity. Advanced Materials, 2016, 28, 3683-3689.	21.0	396
125	Heterostructures based on two-dimensional layered materials and their potential applications. Materials Today, 2016, 19, 322-335.	14.2	469
126	Photoluminescence Enhancement and Structure Repairing of Monolayer MoSe ₂ by Hydrohalic Acid Treatment. ACS Nano, 2016, 10, 1454-1461.	14.6	179

#	Article	IF	CITATIONS
127	Photoluminescence Enhancement in Defect Monolayer MoSe2 by Hydrohalic Acid Treatment. , 2016, , .		0
128	Synthesis and structure of two-dimensional transition-metal dichalcogenides. MRS Bulletin, 2015, 40, 566-576.	3.5	43
129	MoS2 Surface Structure Tailoring via Carbonaceous Promoter. Scientific Reports, 2015, 5, 10378.	3.3	28
130	Monitoring Morphological Changes in 2D Monolayer Semiconductors Using Atom-Thick Plasmonic Nanocavities. ACS Nano, 2015, 9, 825-830.	14.6	101
131	Epitaxial growth of a monolayer WSe ₂ -MoS ₂ lateral p-n junction with an atomically sharp interface. Science, 2015, 349, 524-528.	12.6	1,009
132	Designed hybrid nanostructure with catalytic effect: beyond the theoretical capacity of SnO2 anode material for lithium ion batteries. Scientific Reports, 2015, 5, 9164.	3.3	119
133	Emerging energy applications of two-dimensionalÂlayered transition metal dichalcogenides. Nano Energy, 2015, 18, 293-305.	16.0	236
134	A novel single-layered MoS ₂ nanosheet based microfluidic biosensor for ultrasensitive detection of DNA. Nanoscale, 2015, 7, 2245-2249.	5.6	100
135	Recent advances in controlled synthesis of two-dimensional transition metal dichalcogenides via vapour deposition techniques. Chemical Society Reviews, 2015, 44, 2744-2756.	38.1	709
136	Printed all-solid flexible microsupercapacitors: towards the general route for high energy storage devices. Nanotechnology, 2014, 25, 094010.	2.6	100
137	Hybrid CuO/SnO2 nanocomposites: Towards cost-effective and high performance binder free lithium ion batteries anode materials. Applied Physics Letters, 2014, 105, .	3.3	53
138	Real-time, sensitive electrical detection ofCryptosporidium parvumoocysts based on chemical vapor deposition-grown graphene. Applied Physics Letters, 2014, 104, 063705.	3.3	3
139	Excitons in a mirror: Formation of "optical bilayers―using MoS2 monolayers on gold substrates. Applied Physics Letters, 2014, 104, .	3.3	31
140	Pre-lithiation of onion-like carbon/MoS ₂ nano-urchin anodes for high-performance rechargeable lithium ion batteries. Nanoscale, 2014, 6, 8884-8890.	5.6	93
141	Dual Wavelength Electroluminescence from CdSe/CdS Tetrapods. ACS Nano, 2014, 8, 2873-2879.	14.6	56
142	CoO nanoflowers woven by CNT network for high energy density flexible micro-supercapacitor. Nano Energy, 2014, 3, 46-54.	16.0	185
143	Catalyst engineering for lithium ion batteries: the catalytic role of Ge in enhancing the electrochemical performance of SnO ₂ (GeO ₂) _{0.13} /G anodes. Nanoscale, 2014, 6, 15020-15028.	5.6	26
144	3D graphene supported MoO ₂ for high performance binder-free lithium ion battery. Nanoscale, 2014, 6, 9839-9845.	5.6	82

#	Article	IF	CITATIONS
145	Phase Transformation Induced Capacitance Activation for 3D Grapheneâ€CoO Nanorod Pseudocapacitor. Advanced Energy Materials, 2014, 4, 1301788.	19.5	83
146	Application of solvent modified PEDOT:PSS to graphene electrodes in organic solar cells. Nanoscale, 2013, 5, 8934.	5.6	61
147	Large scale synthesized sulphonated reduced graphene oxide: a high performance material for electrochemical capacitors. RSC Advances, 2013, 3, 14954.	3.6	16
148	Synthesis and Transfer of Single-Layer Transition Metal Disulfides on Diverse Surfaces. Nano Letters, 2013, 13, 1852-1857.	9.1	612
149	Preparation of MoS ₂ oated Threeâ€Đimensional Graphene Networks for Highâ€Performance Anode Material in Lithiumâ€ion Batteries. Small, 2013, 9, 3433-3438.	10.0	542
150	Large-Area 2-D Electronics: Materials, Technology, and Devices. Proceedings of the IEEE, 2013, 101, 1638-1652.	21.3	46
151	Selective Decoration of Au Nanoparticles on Monolayer MoS2 Single Crystals. Scientific Reports, 2013, 3, 1839.	3.3	380
152	Intrinsic Structural Defects in Monolayer Molybdenum Disulfide. Nano Letters, 2013, 13, 2615-2622.	9.1	1,766
153	Chapter 3. Photoelectrical Responses of Carbon Nanotube–Polymer Composites. RSC Nanoscience and Nanotechnology, 2013, , 51-71.	0.2	0
154	Self-assembly of hierarchical MoSx/CNT nanocomposites (2 <x<3): 2013,="" 2169.<="" 3,="" anode="" batteries.="" for="" high="" ion="" lithium="" materials="" performance="" reports,="" scientific="" td="" towards=""><td>3.3</td><td>290</td></x<3):>	3.3	290
155	Growth selectivity of hexagonal-boron nitride layers on Ni with various crystal orientations. RSC Advances, 2012, 2, 111-115.	3.6	72
156	Synthesis and Characterization of Hexagonal Boron Nitride Film as a Dielectric Layer for Graphene Devices. ACS Nano, 2012, 6, 8583-8590.	14.6	472
157	Integrated Circuits Based on Bilayer MoS ₂ Transistors. Nano Letters, 2012, 12, 4674-4680.	9.1	1,526
158	Single-Layer MoS ₂ Phototransistors. ACS Nano, 2012, 6, 74-80.	14.6	3,103
159	Synthesis of Monolayer Hexagonal Boron Nitride on Cu Foil Using Chemical Vapor Deposition. Nano Letters, 2012, 12, 161-166.	9.1	1,057
160	van der Waals Epitaxy of MoS ₂ Layers Using Graphene As Growth Templates. Nano Letters, 2012, 12, 2784-2791.	9.1	888
161	Growth of Large-Area and Highly Crystalline MoS ₂ Thin Layers on Insulating Substrates. Nano Letters, 2012, 12, 1538-1544.	9.1	1,749
162	Chemically modified graphene: flame retardant or fuel for combustion?. Journal of Materials Chemistry, 2011, 21, 3277-3279.	6.7	70

Yumeng Shi

#	Article	IF	CITATIONS
163	Graphene Oxide as a Carbon Source for Controlled Growth of Carbon Nanowires. Small, 2011, 7, 1199-1202.	10.0	75
164	Preparation of Novel 3D Graphene Networks for Supercapacitor Applications. Small, 2011, 7, 3163-3168.	10.0	980
165	Electrical Detection of DNA Hybridization with Singleâ€Base Specificity Using Transistors Based on CVDâ€Grown Graphene Sheets. Advanced Materials, 2010, 22, 1649-1653.	21.0	516
166	Aromatic Molecules Doping in Single-Layer Graphene Probed by Raman Spectroscopy and Electrostatic Force Microscopy. Japanese Journal of Applied Physics, 2010, 49, 01AH04.	1.5	10
167	Synthesis of Few-Layer Hexagonal Boron Nitride Thin Film by Chemical Vapor Deposition. Nano Letters, 2010, 10, 4134-4139.	9.1	1,058
168	Work Function Engineering of Graphene Electrode <i>via</i> Chemical Doping. ACS Nano, 2010, 4, 2689-2694.	14.6	501
169	Nanoelectronic biosensors based on CVD grown graphene. Nanoscale, 2010, 2, 1485.	5.6	408
170	Enhancing the conductivity of transparent graphene films via doping. Nanotechnology, 2010, 21, 285205.	2.6	321
171	Effective doping of single-layer graphene from underlying <mml:math xmlns:mml="http://www.w3.org/1998/Math/MathML" display="inline"><mml:mrow><mml:msub><mml:mrow><mml:mtext>SiO</mml:mtext></mml:mrow><mml:mn> Physical Review B. 2009. 79</mml:mn></mml:msub></mml:mrow></mml:math 	•2<⁄¦mml:r	nn>
172	Doping Single‣ayer Graphene with Aromatic Molecules. Small, 2009, 5, 1422-1426.	10.0	537
173	Photoelectrical Response in Single‣ayer Graphene Transistors. Small, 2009, 5, 2005-2011.	10.0	141
174	Symmetry Breaking of Graphene Monolayers by Molecular Decoration. Physical Review Letters, 2009, 102, 135501.	7.8	224
175	White organic light emitting devices with thin 4-(dicyanomethylene)-2-t-butyl-6(1,1,7,7-tetramethyljulolidyl-9-enyl)-4H-pyran (DCJTB) layer. Displays, 2008, 29, 419-423.	3.7	6
176	Emission mechanism in the terbium complex doped PVK system. Frontiers of Optoelectronics in China, 2008, 1, 130-133.	0.2	1
177	Work function engineering of electrodes via electropolymerization of ethylenedioxythiophenes and its derivatives. Organic Electronics, 2008, 9, 859-863.	2.6	30
178	Multilayer cathode for organic light-emitting devices. Displays, 2008, 29, 323-326.	3.7	0
179	Label-Free Electronic Detection of DNA Using Simple Double-Walled Carbon Nanotube Resistors. Journal of Physical Chemistry C, 2008, 112, 9891-9895.	3.1	37
180	Differentiation of Gas Molecules Using Flexible and All-Carbon Nanotube Devices. Journal of Physical Chemistry C, 2008, 112, 650-653.	3.1	85

#	Article	IF	CITATIONS
181	Photoresponse in Self-Assembled Films of Carbon Nanotubes. Journal of Physical Chemistry C, 2008, 112, 13004-13009.	3.1	24
182	Photoconductivity from Carbon Nanotube Transistors Activated by Photosensitive Polymers. Journal of Physical Chemistry C, 2008, 112, 18201-18206.	3.1	17
183	Interaction between fluorene-based polymers and carbon nanotubes/carbon nanotube field-effect transistors. , 2008, , .		0
184	Effects of substrates on photocurrents from photosensitive polymer coated carbon nanotube networks. Applied Physics Letters, 2008, 92, .	3.3	9
185	N-type behavior of ferroelectric-gate carbon nanotube network transistor. Applied Physics Letters, 2008, 93, 082103.	3.3	11
186	Heme-Enabled Electrical Detection of Carbon Monoxide at Room Temperature Using Networked Carbon Nanotube Field-Effect Transistors. Chemistry of Materials, 2007, 19, 6059-6061.	6.7	16
187	Poly(3,3‴-didodecylquarterthiophene) field effect transistors with single-walled carbon nanotube based source and drain electrodes. Applied Physics Letters, 2007, 91, 223512.	3.3	26
188	Quantum well organic light emitting diodes with ultra thin Rubrene layer. Displays, 2007, 28, 97-100.	3.7	7
189	Electroluminescence characteristics of a new kind of rare-earth complex: TbY(o-MOBA)6(phen)22H2O. Journal of Luminescence, 2007, 122-123, 272-274.	3.1	7
190	Electroluminescent devices based on rare-earth complex TbY(p-MBA)6(phen)2. Journal of Luminescence, 2007, 122-123, 671-673.	3.1	12
191	Organic light-emitting diodes with improved hole–electron balance and tunable light emission with aromatic diamine/bathocuproine multiple hole-trapping-layer. Displays, 2006, 27, 166-169.	3.7	14
192	Synthesis of Transition Metal Dichalcogenides. , 0, , 344-358.		0
193	Performance Limits and Potential of Multilayer Graphene–Tungsten Diselenide Heterostructures. Advanced Electronic Materials, 0, , 2100355.	5.1	2